

Impact of a Pioneer/Rindler-type acceleration on the Oort cloud

Lorenzo Iorio¹

Ministero dell'Istruzione, dell'Università e della Ricerca (M.I.U.R.)-Istruzione

Fellow of the Royal Astronomical Society (F.R.A.S.)

International Institute for Theoretical Physics and High Mathematics Einstein-Galilei

Permanent address for correspondence: Viale Unità di Italia 68, 70125, Bari (BA), Italy

`lorenzo.iorio@libero.it`

Received _____; accepted _____

ABSTRACT

According to a recent modified model of gravity at large distances, a radial constant and uniform extra-acceleration $\mathbf{A}_{\text{Rin}} = A_{\text{Rin}}\hat{\mathbf{r}}$ of Rindler type acts upon a test particle p in the static field of a central mass M if certain conditions are satisfied. Among other things, it was proposed as a potentially viable explanation of a part of the Pioneer anomaly. We study the impact that an anomalous Rindler-type term as large as $|A_{\text{Rin}}| \sim 10^{-10} \text{ m s}^{-2}$ may have on the orbital dynamics of a typical object of the Oort cloud whose self-energy is quite smaller than its putative Rindler energy. By taking a typical comet moving along a highly eccentric and inclined orbit throughout the expected entire extension of the Oort cloud ($\sim 0.02 \text{ pc} - 1 \text{ pc}$), it turns out that the addition of an outward Rindler-like acceleration, i.e. for $A_{\text{Rin}} > 0$, does not allow bound orbits. Instead, if $A_{\text{Rin}} < 0$, the resulting numerically integrated trajectory is limited in space, but it radically differs from the standard Keplerian ellipse. In particular, the heliocentric distance of the comet gets markedly reduced and experiences high frequency oscillations, its speed is increased, and the overall pattern of the trajectory is quite isotropic. As a consequence, the standard picture of the Oort cloud is radically altered since its modified orbits are much less sensitive to the disturbing actions of the Galactic tide and nearby passing stars whose effects, in the standard scenario, are responsible for the phenomenology on which our confidence in the existence of the cloud itself is based. The present analysis may be supplemented in future by further statistical Monte Carlo-type investigations by randomly varying the initial conditions of the comets.

Subject headings: Experimental studies of gravity; Experimental tests of gravitational theories; Modified theories of gravity; Oort cloud; Orbital and rotational dynamics

PACS: 04.80.-y; 04.80.Cc; 04.50.Kd; 96.50.Hp; 96.25.De

1. Introduction

Recently, Grumiller (2010), under certain assumptions, put forth a quite general model for the gravitational field of a static central object of mass M at large distances r from it. As a result, the acceleration felt by a test particle p in the field of M turns out to be modified by the appearance of a Rindler-type additional term. Thus, the total acceleration becomes (Grumiller 2010; Carloni et al. 2011; Grumiller & Preis 2011)

$$\mathbf{A} = -\frac{GM}{r^2}\hat{\mathbf{r}} + \mathbf{A}_{\text{Rin}}, \quad (1)$$

where G is the Newtonian gravitational constant, and

$$\mathbf{A}_{\text{Rin}} = A_{\text{Rin}}\hat{\mathbf{r}} : \quad (2)$$

the sign of A_{Rin} is left indeterminate by the theory. Notice that Grumiller & Preis (2011) assumed that A_{Rin} is a universal constant. Concerning its sign and magnitude, Grumiller & Preis (2011) took

$$A_{\text{Rin}} = -1 \times 10^{-10} \text{ m s}^{-2}. \quad (3)$$

Importantly, Carloni et al. (2011); Grumiller & Preis (2011) argued that, if eq. (1) has to be valid for a given physical system, then the following condition

$$\frac{Gm_p}{d_p} \lesssim |A_{\text{Rin}}| r \quad (4)$$

must be fulfilled. In eq. (4) m_p and d_p are the mass and a typical size of the test particle p , respectively. Otherwise, the self-energy of the test particle would overwhelm the Rindler energy, and the consequent particle's backreaction on the background would not be negligible. In this case, it would not be possible to assume the universal (=maximal) value for the Rindler acceleration. For more details, see the discussion in Section V of Carloni et al. (2011). Actually, it is easy to show that eq. (4) is not valid for the planets of the solar system since it is

$$\frac{Gm_p}{d_p |A_{\text{Rin}}| r} = \frac{(6 \times 10^2 - 1 \times 10^5) \text{ kau}}{r}, \quad (5)$$

where $1 \text{ kau} = 1000 \text{ astronomical units} = 4.85 \times 10^{-3} \text{ pc}$. Carloni et al. (2011); Grumiller & Preis (2011) noticed that eq. (4) is, instead, fully satisfied for the Pioneer 10/11 probes, affected by the well known Pioneer anomaly (Anderson et al. 1998,

2002) which may partly be explained by the Rindler-type acceleration (Grumiller 2010; Carloni et al. 2011; Grumiller & Preis 2011). Carloni et al. (2011) obtained the following constraint

$$|A_{\text{Rin}}| \lesssim 3 \times 10^{-9} \text{ m s}^{-2} \quad (6)$$

from the propagation of electromagnetic waves, for which the previous caveat is not a concern.

Actually, the solar system host several natural objects orbiting the Sun for which eq. (4) holds: they reside in the Oort cloud (Öpik 1932; Oort 1950). It is a reservoir of frozen cometary nuclei which is supposedly located in the remote peripheries of the solar system. It should be a remnant of the early stages of the formation of the solar system, and it likely formed as a consequence of scattering of planetesimals by the giant planets (Duncan et al. 1987; Higuchi et al. 2006). The Oort cloud has likely a spheroidal shape (Weissman 1996) and a size ranging from about 5 – 10 kau up to 150 – 200 kau (Levison & Donnes 2007). Its existence was conjectured by noticing that the typical lifetimes of comets near the Sun is of the order of $10^4 - 10^5$ yr (Levison & Duncan 1994) due to non-gravitational (sublimation) and gravitational (strong interactions with planets) phenomena, while the age of the solar system is 4 – 5 orders of magnitude larger. Thus, a continuous resupplying from a much more remote, longer-lived source should take place in order to maintain the cometary population in a steady state, as it is observed. Long-period¹ ($P_b \geq 200$ yr) comets, characterized by highly inclined and eccentric orbits (Morbideilli 2005), would originate just from the Oort cloud (Morbideilli 2005; Duncan 2008). They are injected into observable orbits in the planetary regions of the solar system by gravitational interactions with interstellar medium (Stern 1990) and giant molecular clouds (Mazeeva 2004; Jakubík & Neslušan 2008), nearby passing stars (Hills 1981; Bobylev 2010a,b) and the Galactic tide (radial and vertical) (Rickman et al. 2008; Masi et al. 2009): as a result, comet showers may occur (Heisler et al. 1987; Matese et al. 1995). Also other existing minor objects of the solar system like Centaurs, highly elliptical trans-Neptunian objects and Jupiter-family comet population may come from the Oort cloud (Emelyanenko et al. 2007). Connections of terrestrial cratering with such cometary showers originating from the Oort cloud have been investigated by some researchers (Wickramasinghe & Napier 2008).

By taking the Halley² comet as representative, a typical Oort object p may be thought as characterized by a mass (Cevolani et al. 1987)

$$m_p = 2.2 \times 10^{14} \text{ kg} \quad (7)$$

¹The threshold of 200 yr was chosen mainly for historical reasons: it is arbitrary (Morbideilli 2005).

²Although $P_b = 75.3$ yr, its orbital characteristics point towards a capture from the long-period population of the Oort cloud (Fernández 2002).

and mean size (Lamy et al. 2004)

$$d_p = 11 \text{ km}, \quad (8)$$

with a mean density of (Sagdeev et al. 1988)

$$\rho_p = 0.6 \text{ g cm}^{-3}, \quad (9)$$

although uncertainties in several parameters and assumptions (Peale 1989) may lead to a range of values as large as

$$\rho_p = 0.2 - 1.5 \text{ g cm}^{-3}. \quad (10)$$

Such figures and eq. (3) imply that

$$\frac{Gm_p}{d_p |A_{\text{Rin}}| r} = \frac{0.0892 \text{ au}}{r}. \quad (11)$$

Thus, the condition eq. (4) is fully satisfied over the entire extension of the Oort cloud also for bodies which can be much larger and denser than a typical cometary nucleus. Indeed, eq. (4) can approximately be posed as

$$\frac{\pi G \rho_p d_p^2}{|A_{\text{Rin}}| r} \lesssim 1; \quad (12)$$

for, say, $\rho_p = 5 \text{ g cm}^{-3}$, which is the mean density³ of the rocky planets (McFadden et al. 2007), and $d_p = 250 \text{ km}$ we would have

$$\frac{\pi G \rho_p d_p^2}{|A_{\text{Rin}}|} = 4.4 \text{ kau}. \quad (13)$$

In this paper we will explore the consequences that the existence of a Rindler-type extra-acceleration, with the characteristic of eq. (2) and eq. (3), would have on the orbital motion of a typical Oort cloud object. Should the resulting orbital pattern radically differ from the standard Newtonian one, shadows on the Rindler-like acceleration would be casted since the entire dynamical history of the Oort cloud should be re-written and all the inferences nowadays accepted, based on the Newtonian picture of the Oort cloud and of its interaction with the surrounding stellar and Galactic environment, would not be valid anymore. Actually, non-negligible modifications of the Newtonian orbits are expected since the mean Newtonian accelerations A_N of an Oort comet may range from $A_N = 2 \times 10^{-10} \text{ m s}^{-2}$ ($r = 5 \text{ kau}$) to $A_N = 1.5 \times 10^{-13} \text{ m s}^{-2}$ ($r = 200 \text{ kau}$). Concerning general relativity, it will not be considered in the rest of the paper since its effects are

³Clearly, it is highly unlikely that such dense bodies can really exist in the Oort cloud.

totally negligible in the present context. Suffices it to say that the 1PN term of order $\mathcal{O}(c^{-2})$ causes a comet acceleration as small as

$$A_{\text{1PN}} \sim \frac{(GM)^2}{c^2 r^3} \lesssim 10^{-21} \text{ m s}^{-2}, \quad (14)$$

where c is the speed of light in vacuum. As we will see in Figure 2 (Section 2.1), no special relativistic effects will come into play since, although generally increased by the Rindler acceleration, the speed of the Oort comet will remain several orders of magnitude smaller than c .

The plan of the paper is as follows. In Section 2 we numerically compute the trajectory of a typical Oort object for inward (Section 2.1) and outward (Section 2.2) directions of \mathbf{A}_{Rin} . In Section 3 we investigate if an Oort comet acted upon by a Rindler-type acceleration is sensitive to the perturbing actions of the Galactic tide (Section 3.1) and of nearby passing stars (Section 3.2) which, in the standard Newtonian scenario, cause the phenomenology on which our confidence in the existence of the Oort cloud is based. In Section 4 we summarize and discuss our findings.

2. Numerically produced orbits of Oort comets affected by the Rindler acceleration

2.1. An inward Rindler acceleration

The orbital effects of eq. (2)-eq. (3) on an Oort comet p cannot be computed perturbatively since, according to eq. (3), the magnitude of A_{Rin} is of the same order of magnitude of, or larger than the Newtonian acceleration experienced by p .

Thus, we numerically integrate the modified equations of motion of p in a heliocentric frame endowed with cartesian coordinates. We adopt initial conditions, shown in Table 1, such that, in the limit $A_{\text{Rin}} \rightarrow 0$, the resulting orbit reduces to a standard Keplerian ellipse. It is characterized by large values of its eccentricity e and inclination I to the reference $\{x, y\}$ plane, and the semi-major axis a is chosen in such a way that the comet’s motion covers almost all the expected extension of the Oort cloud. The other standard Keplerian orbital elements are the longitude of the ascending node Ω , the argument of pericenter ω and the true anomaly f . The results of the integrations are displayed in Figure 1 and Figure 2 in which the features of the Keplerian ellipse corresponding to the initial conditions of Table 1 are shown in blue for comparison. The qualitative differences with the Newtonian case are striking: bound trajectories still occur, but they radically differ from the Newtonian ones. It is important to note that the condition of eq. (4) is always fulfilled, as shown by the right panel of Figure 2. This is a relevant point since, in principle, it may happen that the comet enters a region in which its gravitational self-energy becomes larger than its putative Rindler energy, thus destroying the validity of the approach followed which

Table 1: Initial conditions, in kau and $\text{kau Myr}^{-1} = 4.74 \text{ m s}^{-1}$, adopted for the numerical integration of the modified equations of motion of an Oort comet acted upon by the Rindler-type acceleration of eq. (2). In terms of standard Newtonian mechanics, they correspond to a Keplerian ellipse with $a = 102.507 \text{ kau}$, $e = 0.955$, $I = 77.41 \text{ deg}$, $\Omega = -139.87 \text{ deg}$, $\omega = 321.94 \text{ deg}$, $f = -152.14 \text{ deg}$. The orbital period $P_b = 32.81 \text{ Myr}$. The perihelion distance is $q \doteq a(1 - e) = 4.606 \text{ kau}$, and the aphelion distance is $Q \doteq a(1 + e) = 200.407 \text{ kau}$.

$x_0 \text{ (kau)}$	$y_0 \text{ (kau)}$	$z_0 \text{ (kau)}$	$\dot{x}_0 \text{ (kau Myr}^{-1}\text{)}$	$\dot{y}_0 \text{ (kau Myr}^{-1}\text{)}$	$\dot{z}_0 \text{ (kau Myr}^{-1}\text{)}$
45	35	10	−23	−15	−15

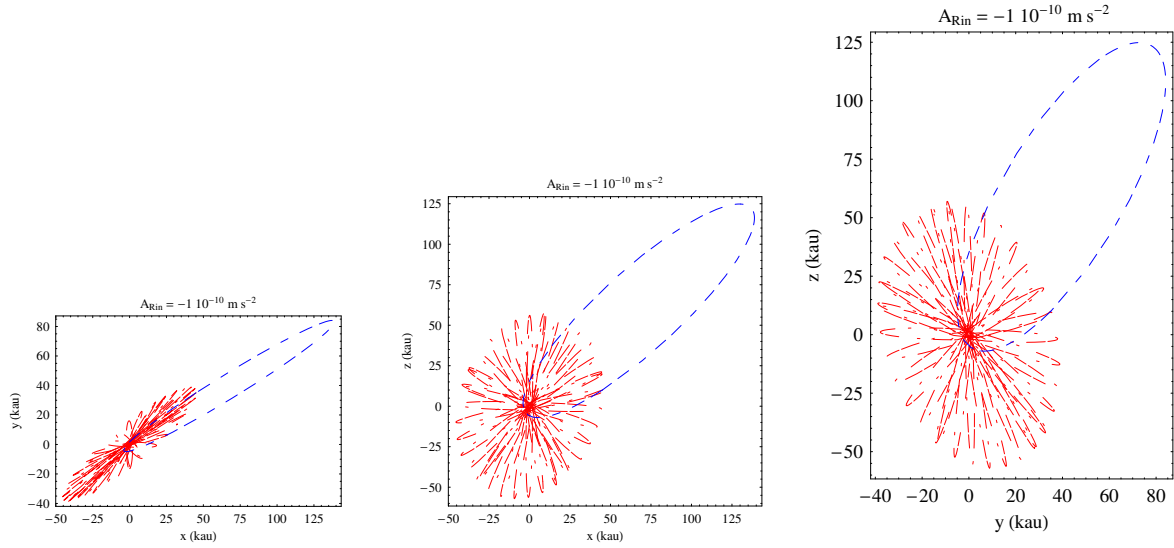


Fig. 1.— Sections in the coordinates planes of the numerically integrated orbits for the Oort comet of Table 1 over one Keplerian orbital period P_b . The dash-dotted red lines are the projections of the modified orbit by assuming that the Rindler acceleration is directed towards the Sun. The dashed blue lines are the projections of the Keplerian ellipse.

was implemented by keeping $A_{\text{Rin}} \neq 0$ throughout the whole integration. As anticipated in Section 1, the non-relativistic treatment is justified by the smallness of the comet's speed v , displayed in the middle panel of Figure 2. Globally, the heliocentric distance r is strongly reduced, especially in the regions which in the Newtonian case correspond to the aphelion: the minimum distance suffers a relatively smaller reduction with respect to the Newtonian case. Indeed, the left panel of Figure 2 tells us that, in the Rindler case, r oscillates with high frequency between about 2 kau and 50 kau.

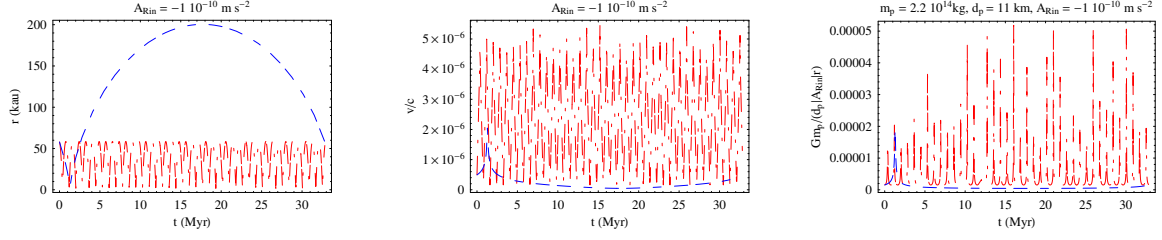


Fig. 2.— Heliocentric distances, in kau, velocities, in units of c , and ratio $Gm_p/(d_p |A_{\text{Rin}}| r)$ of the numerically integrated orbits for the Oort comet of Table 1 over one Keplerian orbital period P_b . The dash-dotted red lines refer to the modified orbit by assuming that the Rindler acceleration is directed towards the Sun. The dashed blue lines refer to the Keplerian ellipse.

2.2. An outward Rindler acceleration

If the Rindler-type acceleration is radially directed from the Sun to the comet, no bounds orbit may exist, as depicted by Figure 3 which refers to the same initial conditions of Table 1. We adopted decreasing values of A_{Rin} with respect to $|A_{\text{Rin}}| = 1 \times 10^{-10} \text{ m s}^{-2}$,

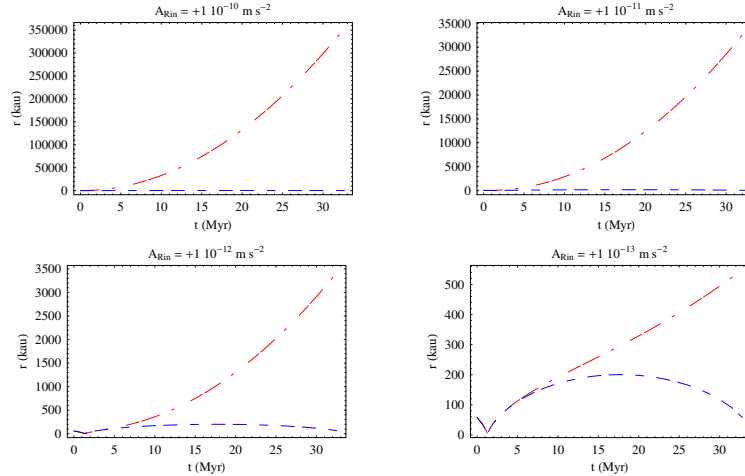


Fig. 3.— Numerically integrated heliocentric distances r , in kau, of the modified trajectory (dash-dotted red lines) of an Oort comet with the initial conditions of Table 1 for decreasing positive values of A_{Rin} . The duration of the integration is one Keplerian orbital period P_b .

but the result is substantially the same.

3. Consequences of a Rindler-type acceleration on a perturbed Oort cloud

It seems plausible to expect that the Rindler trajectories are less sensitive than the Newtonian one to those disturbances which affect the Oort cloud yielding those phenomena

which are the basis of our confidence in the existence of the cloud with the features usually attributed to it. If so, the existence of the Rindler acceleration would drastically alter the dynamical history of the Oort cloud.

3.1. The Galactic tide

The effect of the Galactic tide on the orbit of an Oort comet (Heisler & Tremaine 1986) can be obtained from the following expression of the Galactic tidal acceleration (Morbideilli 2005)

$$\begin{aligned} A_x^{(\text{tid})} &= \Omega_0^2 x, \\ A_y^{(\text{tid})} &= -\Omega_0^2 y, \\ A_z^{(\text{tid})} &= -4\pi G \rho_0 z, \end{aligned} \tag{15}$$

where ρ_0 is the mass density in the solar neighborhood and Ω_0 is the frequency of solar revolution around the Galaxy. The expressions of eq. (15) refer to a heliocentric frame with the x axis pointing away from the Galactic center, the y axis in the direction of the Galactic rotation and z axis towards the South Galactic Pole⁴ (Morbideilli 2005). Both visible stars and Dark Matter concur to the local mass density in the solar neighborhood. Concerning the baryonic stellar component, the local mass density of main-sequence stars is (Reid et al. 2002)

$$\rho_{\text{MS}} \sim 0.031 M_\odot \text{ pc}^{-3} = 2.09 \times 10^{-24} \text{ g cm}^{-3}, \tag{16}$$

while, according to the most recent results, the Dark Matter local density in the Galactic solar neighborhood is (de Boer & Weber 2011)

$$\rho_{\text{DM}} = 1.3 \text{ GeV cm}^{-3} = 2.31 \times 10^{-24} \text{ g cm}^{-3}. \tag{17}$$

Thus, we will assume

$$\rho_0 \sim 4 \times 10^{-24} \text{ g cm}^{-3} = 1.5 \times 10^{22} \text{ kg kau}^{-3}. \tag{18}$$

The frequency of the Galactic revolution of the Sun Ω_0 can be evaluated from its circular rotation speed (Reid et al. 2009) $\Theta_0 = 254 \text{ km s}^{-1}$ and its distance to the Galactic center (Reid et al. 2009) $R_0 = 8.4 \text{ kpc}$ as

$$\Omega_0 = \frac{\Theta_0}{R} = 0.0309 \text{ Myr}^{-1}. \tag{19}$$

⁴The Galactic plane is tilted by 62.6 deg to the celestial equator (Sullivan 1984), so that it is almost at right angle to the ecliptic.

Thus, its period of revolution is

$$T_0 = 203.176 \text{ Myr.} \quad (20)$$

In Figure 4 we show the numerically integrated Rindlerian and Newtonian trajectories, including eq. (15), over a full revolution of the Sun around the Galaxy. We used the same initial conditions of Table 1 for the Oort comet. As expected, the differences between the

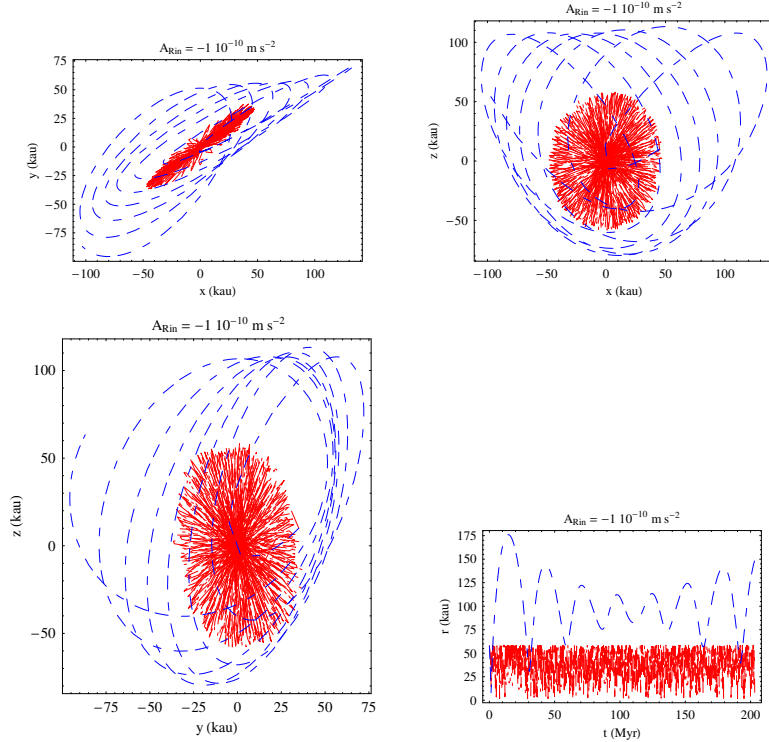


Fig. 4.— Coordinate sections of the numerically integrated trajectories and heliocentric distances r of an Oort comet affected by the Galactic tide of eq. (15) with (dash-dotted red lines) and without (dashed blue lines) the Rindler-type acceleration of eq. (3). The initial conditions of the Oort comet are those of Table 1. The duration of the integration is one full Galactic revolution ($T_0 = 203.176$ Myr).

Newtonian and the modified scenarios are remarkable: a comparison with Figure 1 and Figure 2 shows that the Rindler trajectory is left substantially unaffected by the Galactic tide, contrary to the Newtonian one. It can be shown that also for an outward Rindler acceleration the Galactic tide does not have influence in the sense that the comet does not remain bound, as in Figure 3.

3.2. A close encounter with a passing star

Here we consider the perturbing action of a passing star s with $m_s = M_\odot$ over an unperturbed Keplerian orbital period P_b of the Oort comet. The initial conditions of s are listed in Table 2. In the numerical integration of the equations of motion we assume that

Table 2: Initial conditions, in kau and $\text{kau Myr}^{-1} = 4.74 \text{ m s}^{-1}$, of a perturbing passing star s adopted for the numerical integration of the modified equations of motion of an Oort comet acted upon by the Rindler-type acceleration of eq. (2). They correspond to a heliocentric distance $r_0^{(s)} = 3.2 \text{ pc}$ and a speed $v_0^{(s)} = 0.61 \text{ km s}^{-1}$.

$x_0^{(s)}$ (kau)	$y_0^{(s)}$ (kau)	$z_0^{(s)}$ (kau)	$\dot{x}_0^{(s)}$ (kau Myr $^{-1}$)	$\dot{y}_0^{(s)}$ (kau Myr $^{-1}$)	$\dot{z}_0^{(s)}$ (kau Myr $^{-1}$)
270	370	470	−42.18	−63.28	−105.47

s moves uniformly with $v^{(s)}(t) = v_0^{(s)}$. The result is depicted in Figure 5. It can be noticed

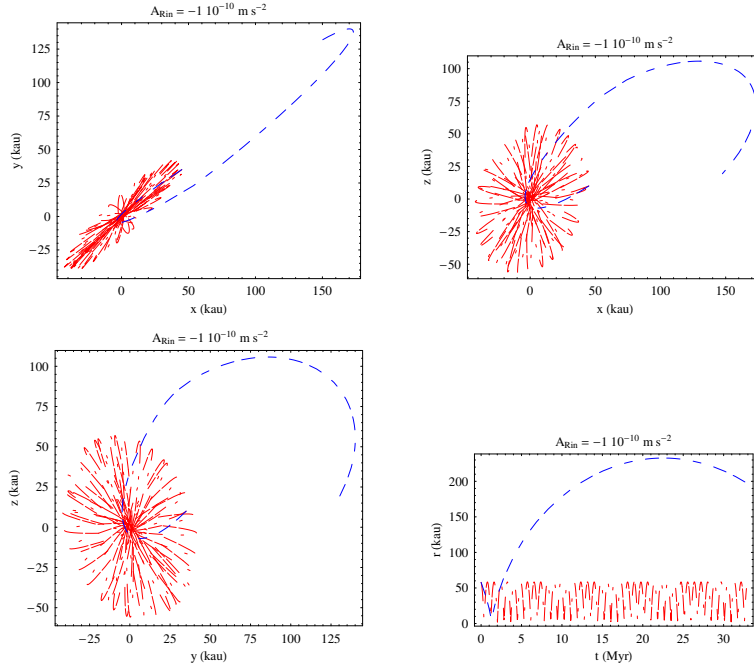


Fig. 5.— Coordinate sections of the numerically integrated trajectories and heliocentric distances r of an Oort comet affected by the passing star of Table 2 with (dash-dotted red lines) and without (dashed blue lines) the Rindler-type acceleration of eq. (3). The initial conditions of the comet are those of Table 1. The duration of the integration is one (unperturbed) Keplerian period P_b .

that, while the Keplerian ellipse is, actually, distorted⁵ by the Newtonian interaction with s , the trajectory computed with the Rindler acceleration remains substantially unaffected. Also in this case, it can be shown that no bound orbits can exist if \mathbf{A}_{Rin} is directed outward.

4. Discussion and conclusions

The analysis performed in this paper should be considered just as a preliminary one. It aims at exploring semi-qualitatively how the presence of an additional radial Rindler-like acceleration may affect the orbital motion of bodies whose self-energy is smaller than their putative Rindler energy like the objects moving in the Oort cloud. We only choose a specific set of initial conditions which correspond, in the Newtonian scenario, to a typical orbital configuration for an Oort comet moving on a highly eccentric and inclined ellipse which almost extends throughout the entire expected extension of the Oort cloud. More refined numerical analyses may explore larger ensembles of initial conditions with a statistical approach. It would also be interesting to repeat Monte Carlo simulations of the dynamical evolution of the Oort cloud over the age of the solar system like, e.g., those by Rickman et al. (2008) and Masi et al. (2009) by explicitly including a Rindler-type extra-acceleration, and inspect how several key features of the cloud change with respect to the usual Newtonian scenario.

In our numerical analysis we found that the standard Newtonian picture is notably altered by an additional radial Rindler acceleration as large as $10^{-10} \text{ m s}^{-2}$ which, in the case of an Oort comet, would not be smaller than the Newtonian one. Bound orbits are not possible if \mathbf{A}_{Rin} is directed outward, even for $A_{\text{Rin}} = 10^{-13} \text{ m s}^{-2}$. Conversely, if the Rindler acceleration is directed from the comet to the Sun the resulting trajectory is limited in space, but it is completely different from a Keplerian ellipse. In particular, the heliocentric distance r is greatly reduced, and it experiences high-frequency variations during a Keplerian orbital period P_b . Moreover, the spatial pattern of the modified trajectory is quite isotropic over P_b . As a consequence, the Rindlerian trajectory is much less sensitive than the Newtonian one to disturbing effects like the Galactic tide and nearby passing stars.

Although, as pointed out above, more extended numerical investigations should be implemented by varying the initial conditions in a Monte Carlo fashion, it is difficult to believe that the main features of the Oort cloud, which lead to a general consensus about its existence, may be preserved by the existence of a Rindler-type extra-acceleration of the order of $10^{-10} \text{ m s}^{-2}$. Our results are not necessarily limited to the specific model by Grumiller (2010): indeed, they are quite general and are valid for any hypothetical constant

⁵In this particular case, the comet is stripped away by the stellar passage: indeed, this is one of the causes of the gradual depletion of the Oort cloud (Remy & Mignard 1985).

and uniform radial acceleration. In the case of the Pioneer anomaly, the magnitude of the anomalous acceleration may be as large as $|A_{\text{Pio}}| \leq 1 \times 10^{-9} \text{ m s}^{-2}$ and all the previous results remain qualitatively valid, being the anomalous behavior of an Oort comet even more remarkable from a quantitative point of view. Finally, we notice that using the Oort cloud may, in principle, be useful also for other long-range modified models of gravity.

REFERENCES

- Anderson J. D. Laing P. A., Lau E. L., Liu A. S., Nieto M. M., Turyshev S. G., 1998, Physical Review Letters, 81, 2858
- Anderson J. D. Laing P. A., Lau E. L., Liu A. S., Nieto M. M., Turyshev S. G., 2002, Physical Review D, 65, 082004
- Bobylev V. V., 2010a, Astronomy Letters, 36, 220
- Bobylev V. V., 2010b, Astronomy Letters, 36, 816
- Carlioni S., Grumiller D., Preis F., 2011, Phys. Rev. D., 83, 124024
- Cevolani G., Bortolotti G., Hajduk A., 1987, Nuovo Cimento C, 10, 587
- de Boer W., Weber M., 2011, J.Cosmol. Astropart. Phys., 04, 002
- Duncan M. J., Quinn T., Tremaine S., 1987, Astron. J., 94, 1330
- Duncan M. J., 2008, Space Sci. Rev., 138, 109
- Emelyanenko V. V., Asher D. J., Bailey M. E., 2007, Mon. Not. of the Royal Astron. Soc., 381, 779
- Fernández J. A., 2002, Earth, Moon and Planets, 89, 325
- Grumiller D., 2010, Phys. Rev. Lett., 105, 211303. Erratum-ibid. 106, 039901
- Grumiller D., Preis F., 2011, honourable mention in 2011 GRF essay contest, arXiv:1107.2373
- Heisler J., Tremaine S., Alcock C., 1987, Icarus, 70, 269
- Heisler J., Tremaine S., 1986, Icarus, 65, 13
- Higuchi A., Kokubo E., Mukai T., 2006, Astron. J., 131, 1119
- Hills J. G., 1981, Astron. J., 86, 1730
- Jakubík M., and Neslušan L., 2008, Contrib. Astron. Obs. Skalnaté Pleso, 38, 33
- Lamy P. L., Toth I., Fernandez Y. R., Weaver H. A., 2004, in Festou M. C., Keller H. U., Weaver H. A., eds., Comets II, University of Arizona Press, Tucson, p. 223
- Levison H. F., Duncan M. J., 1994, Icarus, 108, 18
- Levison H. F., Donnes L., 2007, in McFadden L.-A., Weissman P. R., Johnson T. V., eds., Encyclopedia of the Solar System (2nd ed.). Academic Press, Amsterdam, p. 575

- Masi M., Secco L., Gonzalez G., 2009, *The Open Astronomy Journal*, 2, 74,
- Matese J. J., Whitman P. G., Innanen K. A., Valtonen M. J., 1995, *Icarus*, 116, 255
- Mazeeva O. A., 2004, *Sol. Syst. Res.*, 38, 325
- McFadden L.-A., Weissman P. R., Johnson T. V., eds., 2007, *Encyclopedia of the Solar System* (2nd ed.). Academic Press, Amsterdam
- Morbidelli A., 2005, *astro-ph/0512256*
- Oort J. H., 1950, *Bull. Astron. Inst. Netherlands*, 11, 91
- Öpik E., 1932, *Proc. Am. Acad. Arts Sci.* 67, 169
- Peale S. J., 1989, *Icarus*, 82, 36
- Reid I. N., Gizis J. E., Hawley S. L., 2002, *Astron. J.* 124, 2721
- Reid M. J., Menten K. M., Zheng X. W., Brunthaler A., Moscadelli L., Xu Y., Zhang B., Sato M., Honma M., Hirota T., Hachisuka K., Choi Y. K., Moellenbrock G. A., Bartkiewicz A., 2009, *Astrophys J.*, 700, 137
- Remy F., Mignard F., 1985, *Icarus*, 63, 1
- Rickman H., Fouchard M., Froeschlé C., Valsecchi G. B., 2008, *Celestial Mechanics and Dynamical Astronomy*, 102, 111
- Sagdeev R. Z., Elyasberg P. E., Moroz V. I., 1988, *Nature*, 331, 240
- Stern S. A., 1990, *Icarus*, 84, 447
- Sullivan W. III, ed., 1984, *The Early Years of Radio Astronomy: Reflections Fifty Years after Jansky's Discovery*, Cambridge University Press, London
- Weissman P.R., 1996, *Earth, Moon, and Planets*, 72, 25
- Wickramasinghe J. T., Napier W. M., 2008, *Mon. Not. R. Astron. Soc.*, 387, 153